ELSEVIER

Journal of Nuclear Materials 241–243 (1997) 701–706

journal of nuclear materials

Divertor geometry optimization for ASDEX Upgrade

R. Schneider *, H.S. Bosch, J. Neuhauser, D. Coster, K. Lackner, M. Kaufmann

Max-Planck-Institut für Plasmaphysik, EURATOM Association, D-85748 Garching, Germany

Abstract

One of the critical questions to be solved for ITER (or any other reactor) is the power exhaust problem (compatible with particle exhaust). Optimized divertors have to be tested in existing geometries based mainly on the idea of closing them very efficiently to the main chamber and, by the choice of the plate and baffle geometry, positively influencing the flow pattern of hydrogen favoring good impurity entrainment. Also, for ASDEX Upgrade there is an experimental necessity for an improved divertor due to the increased heating power (24 MW will be available from 1997 on compared to the present 18 MW). We present the optimization strategy for the divertor II of ASDEX Upgrade, using elaborate numerical models and codes (B2-Eirene) as well as simple models. We start with the choice of a proper target plate geometry, and then further discuss how main chamber and private flux baffling will be done, and how this affects neutral recirculation pattern and pumping properties. For the final configuration the impurity entrainment properties are analyzed.

Keywords: ASDEX-Upgrade; 2D model; Fluid simulation; Monte Carlo simulation

1. Introduction

One of the most challenging issues in the design of ITER is that of a divertor concept which simultaneously provides tolerable power loads on the target plates and sufficient particle exhaust. Presently, it seems clear that this requires strong impurity entrainment in the divertor due to very limited core Z_{eff} allowed for in order to obtain an ignited plasma (less than 1.6 for ITER, with 0.4 already accounted for by helium and intrinsic impurities [1]). Therefore, optimized divertors [2–4] have to be tested in existing geometries based mainly on the idea of efficiently closing them to the main chamber and, by the choice of the plate and baffle geometry, positively influencing the flow pattern of hydrogen favoring good impurity entrainment. No validated divertor concept exists so far, which could cope with the extreme power flow levels envisaged for ITER and to be expected in a subsequent DEMO.

Also, for ASDEX Upgrade there is an experimental necessity for an improved divertor [5] due to the increased heating power (24 MW will be available from 1997 onwards compared to actually 18 MW). Currently, 12 MW heating power coupled to the plasma gives power load densities of up to 6 MW/m^2 time averaged and larger than 20 MW/m^2 in the peak for the divertor I configuration.

In this paper, we present the optimization strategy for the divertor II of ASDEX Upgrade, using elaborate numerical models and codes (B2-Eirene) as well as simple models. B2-Eirene [6–9] is able to treat the atomic physics processes as well as complicated geometries involved and has been validated against running experiments (e.g., model validation work for ohmic discharges [10,11], ELM scenarios [12], including CDH [13], impurity divertor compression [14]).

Starting with the choice of a proper target plate geometry, further discussion of main chamber and private flux baffling will be done. For the final configuration the impurity entrainment properties will be analyzed.

2. Effect of target plate geometry

The target plate geometry strongly influences the plasma profiles by controlling the neutral recycling pattern, which in turn has a strong effect on the symmetry and stability of the divertor plasma and finally on the whole edge region.

* Corresponding author. Tel.: +49-89 3299 2204; fax: +49-89 3299 2580; e-mail: sgs@ipp-garching.mpg.de.

PII S0022-3115(96)00590-9

The radial plasma profile is a consequence of two major contributions (which are coupled self-consistently, see e.g., a radially continuous two-chamber model [15]). In the midplane the plasma particle transport is dominated by the anomalous radial diffusion coefficient (a number in the order of 1 m^2/s), and a possible drift velocity. This plasma drift velocity has to be of the order of the radial diffusion coefficient divided by the SOL width giving a typical value of several 10 m/s to become important. The second major contribution is the neutral transport in the divertor, which can also be interpreted as a classical diffusion-drift-type process. The neutrals are created at the plate and do a random walk with a diffusion coefficient proportional to neutral thermal velocity times the mean free path. Neutrals are reflected perpendicular to the plate with a cosine-like distribution. Therefore, the target plate geometry acts as a radial drift term being proportional to the neutral thermal velocity times sine of the target plate inclination.

For high recycling conditions the neutral diffusion coefficient becomes small. However, the target geometry has still a strong effect through its influence on the neutral drift velocity term. For highly inclined target plates (where the sine-factor is close to 1), this drift velocity must only be larger than several m/s to be comparable to the plasma diffusion term, a condition that is usually fulfilled. Therefore, a strong profile effect for the density profile (and consequently for the temperature profile) is expected from a change of the target inclination, if other transport terms like plasma radial drift velocities or cross field transport driven by main chamber recycling (if e.g., toroidal gaps exist) are small.

Using B2-Eirene the existing divertor I is compared with the Lyra and gas bag configuration concerning their detachment properties. As a quantitative measure for detachment we use the integral momentum loss factor from midplane to target plate. It is calculated from the flux integrated ($d\psi$) pressure profiles at the target plate and midplane:

$$f_{\mathrm{mom}} = 1 - \frac{\int_{\mathrm{target\,plate}} p \cdot \left(1 + \gamma M^2\right) d\psi}{\int_{\mathrm{midplane}} p \cdot \left(1 + \gamma M^2\right) d\psi}.$$

In this integral momentum loss factor ($f_{\mathrm{mom}} = 0$ means no momentum loss, f_{mom} values close to 1 means getting closer to complete detachment), the effect of the acceleration at the sheath entrance appears as the factor γM^2 (γ = adiabatic coefficient; in our case 1; M-mach number). For standard conditions (midplane M practically zero, target plate $M = 1$) this results in an additional factor of 0.5 for the pressure drop.

For divertor I the outer divertor plate reflects the neutrals away from the energy carrying zone close to the separatrix and by this blocks indirectly the detachment. Therefore, divertor I detaches strongly asymmetrically (preferentially on the inner divertor: $f_{\mathrm{mom}}^{\mathrm{inner}} = 0.44$, $f_{\mathrm{mom}}^{\mathrm{outer}} = 0.17$). Nevertheless, the power load on the outer target plate is reduced by the large flux expansion close to the

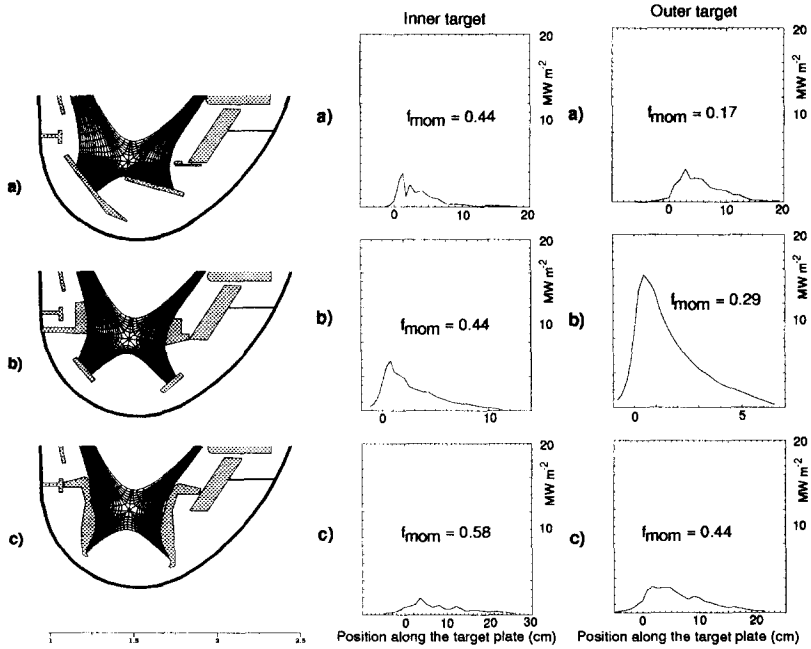

Fig. 1. Computational grids, target plate configurations (left column), inner target (middle column) and outer target (right column) total parallel energy flux density for a: divertor I, b: gasbag and c: Lyra. Total input power is 7.5 MW and separatrix density is $1.0 \cdot 10^{20}$ m^{-3}. f_{mom} is the integral momentum loss factor (see definition in the text).

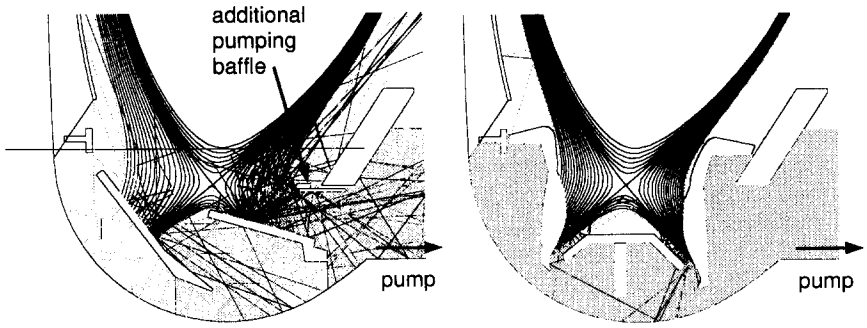

Fig. 2. 100 neutral trajectories for the divertor I and the final Lyra configuration for deuterium atoms (black) and molecules (grey). 50 particles are started from the inner and the outer plate. The midplane conditions were comparable for both cases: 7 MW input power, separatrix density of $3 \cdot 10^{19}$ m^{-3}, similar amount of carbon and neon.

X-point (see Fig. 1). The gas bag is already more symmetric ($f_{\text{mom}}^{\text{inner}} = 0.44$, $f_{\text{mom}}^{\text{outer}} = 0.29$), but has severe problems with power loadings in scenarios without additional external impurities — its perpendicular plates give maximum power loadings (see Fig. 1). The Lyra has for the same density conditions largest and most symmetric momentum losses and lowest power loads ($f_{\text{mom}}^{\text{inner}} = 0.58$, $f_{\text{mom}}^{\text{outer}} = 0.44$, see Fig. 1), because it reflects the neutrals towards the high energy zone at the separatrix and is strongly tilted. Therefore, concerning the operational safety of the machine it offers the best configuration to start with, allowing for scenarios without external impurities and the largest heating power.

In addition to numerical predictions, the different configurations have to be tested experimentally. Therefore, the Divertor II in ASDEX Upgrade is being designed as flexible as possible. There are some cooled base structures on the high and low field sides of the divertor plasma region, which can be equipped with target plates of different shape. The Lyra and gas bag divertors are the basic

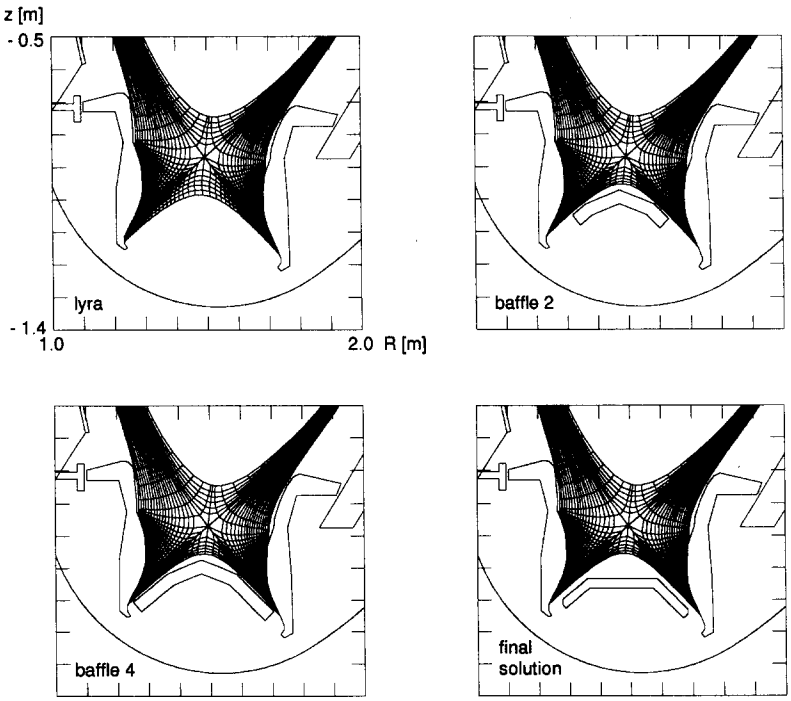

Fig. 3. Three different private flux baffle Lyra configurations (Lyra, Baffle2, Baffle4) used for pumping scan studies plus the final configuration.

configurations in discussion. These can be complemented by various uncooled structures in the private flux region. By opening holes in these baffle structures or even exchanging them one should be able to vary the neutral recycling pattern to test its influence on the divertor performance. After having fixed the target plate geometry (Lyra), the baffling configuration for the first Lyra configuration to be in operation in 1997 has to be designed.

3. Main chamber baffling

Main chamber baffling is necessary to minimize the neutral leakage from the divertor to the main chamber. This is important, because experimentally a deterioration of high confinement for higher neutral fluxes in the main chamber is observed. Additionally, CX sputtering in the main chamber can be a concern (not for ASDEX Upgrade, but probably for ITER).

Fig. 2 shows that divertor I of ASDEX Upgrade is a very open gas-bag like divertor, where the neutrals can penetrate into the whole divertor fan: the baffling towards the main chamber is poor. It has only a small additional pumping baffle, which is not very efficient for the baffling of hydrogen neutrals. However, it gets quite important for the understanding of the compression of neon and helium (see Section 5). Lyra (and gas bag) have a much better reduction of divertor neutral leakage due to its tight baffling up to the X-point. The leakage is reduced by 2 to 3 orders of magnitude for attached or partially detached conditions. Therefore, in contrast to divertor I where main chamber recycling and divertor leakage are equal to each other, now the main chamber recycling is dominant. For the engineering realization, one has to avoid toroidal gaps to the vessel which would produce indirect main chamber leakage.

4. Private flux baffle optimization

After having fixed the target geometry and main chamber baffling, the final step is the optimization of the private flux baffles (Fig. 3).

By changing the private flux baffling the neutral recirculation pattern — especially the neutral penetration to the X-point — is strongly affected and one is even able to suppress flow reversal zones in the hydrogenic flow pattern. These occur usually for high recycling conditions due to strong local ionization sources, resulting in incompatible divertor versus midplane profiles and forcing backflow. This suppression of flow reversal may also lead to better impurity entrainment (to be tested, see later discussion). Density scans for different private flux baffle configurations show little change of detachment properties, but much higher neutral divertor fluxes and there-fore better pumping in the case of optimized baffle length (Baffle 4,

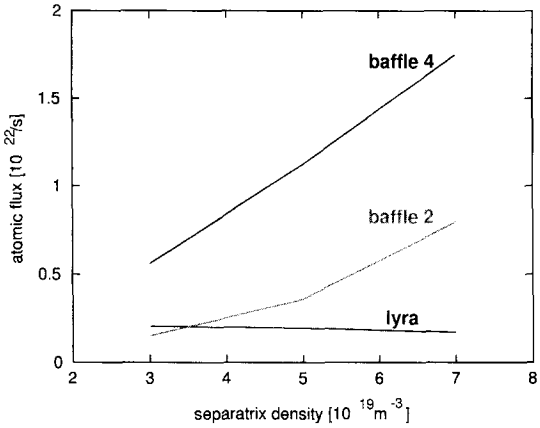

Fig. 4. B2-Eirene results for pumping flux versus separatrix density for three different Lyra configurations (Lyra, Baffle2, Baffle4). Input power is 5 MW.

Fig. 4). This can be easily understood, because by closing most of the private flux region with baffles the very effective plasma pumping is strongly reduced. The distance of the baffle to the plate has to be long enough so that the hydrogen neutrals are still able to escape into the private flux area.

The detachment properties are not changed, because they are more determined by quasi-1D balances along the fieldlines close to the plate, which are not affected strongly by these private flux baffles.

For the realization of the final geometry, the optimized baffle length (baffle 4, see Fig. 3) was used, however the top part (close to the X-point) no longer follows the field line geometry, but is horizontal. By this, it is possible in the experiments to use this private flux baffle (at least transiently or for reduced input power) as a target plate, a necessity for advanced scenarios with high triangularities. The flexibility for testing different neutral recirculation is still achieved by possible holes in the baffle structure for neutral recirculation or additional septum structures for separation of the inner and outer divertors. Also, one can move the plasma separatrix away from the baffle to do experimental scans with quite different private flux divertor baffling: an effective baffle along a fieldline has to be 3 to 4 times the mean free path of the neutrals; opening a gap drastically reduces its baffling effect.

5. Impurity compression

As mentioned before, one critical point for a successful divertor scheme is the existence of strong impurity entrainment.

Analyzing the impurity transport, we use two quantities. The first one is compression, which is the ratio between the neutral density in the pump duct and the average ion midplane density close to the separatrix. The

ratio of impurity compression to hydrogen compression defines the second quantity, which is the enrichment factor. Doing multifluid calculations based on model validation results of the existing divertor I configuration [14], one gets for the final Lyra configuration (as well as for the open Lyra and the inner orthogonal divertor I) a much better compression of helium (an enrichment of helium of typically 2 is now observed in the pumping duct location) than for divertor I (enrichment factors for helium between 0.1 and 0.4). The very good compression of neon in the outside tilted divertor I (enrichment of 1 to 6) is reduced to practically the same as the hydrogen compression (enrichment 1 to 1.5), but is still large enough for effective feedback control.

This prediction is also a crucial test of the predictive quality of the 2D simulations.The difference between the compressions for divertor I and the final Lyra configurations is due to the fact, that the pumping duct recycling cycle is quite different. Neutrals are created at the target plate. If they are able to escape into the pumping duct, they are coming back to the plasma fan as colder neutrals due to collisions with the walls in the duct. That means, they are ionizing further outwards and by this enhance the flux of neutrals being able to escape into the pumping duct (a second particle flux maximum at the plate is created [14]). In the case of the divertor I configuration the pumping duct recycling takes place in the outer SOL part. Its radial extension characterized by one mean free path of the impurity neutrals and the second particle flux maximum at the plate is shifted well apart from the separatrix. Neutrals being ionized in this region are kept in the divertor, because of the forward-streaming of the deuterium background plasma: thermal forces are unimportant in this far outer region, because the power losses creating large temperature gradients occur in the other part of the SOL close to the separatrix. For the compression behavior the existence of the additional pumping baffle at the outer divertor is quite important (see Fig. 2) The worse compression of helium compared to neon is just due to its longer mean free path which produces a larger leakage out of the pumping duct into the main chamber.

In the Lyra the pumping duct recycling cycle is now in the dome region close to the separatrix. Due to the higher electron densities there, creation of impurity neutrals at the plate and reionization of colder neutrals from the dome occur at practically the same position. The better compression of helium in the Lyra is then due to the fact that the helium neutral atoms have longer mean free paths than neon and are therefore easier escaping from the target plate into this dome and from there into the pump.

6. Summary

One of the most challenging issues in the design of ITER is a divertor concept which simultaneously provides tolerable power loads on the target plates and sufficient particle exhaust. A critical test of the influence of target plate geometry and baffling on the divertor performance will be possible with the new ASDEX Upgrade divertor II (together with comparisons of other new generation divertors in JET or DIII-D).

For the optimization process the first step is the target plate geometry, which strongly influences the plasma profiles by controlling the neutral recycling pattern, which in turn has a strong influence on the symmetry and stability of the divertor plasma and finally on the whole edge region. The most symmetric detachment and lowest power loads are found for the Lyra (it reflects the neutrals towards the high energy zone at the separatrix and is strongly tilted). Therefore, concerning operational safety, it offers the best configuration to start with. However, as an option for the future an open gas bag geometry can also be tested. For both options a very tight divertor baffling to the main chamber is foreseen.

The next step is the optimization of the private flux baffling, which affects strongly the penetration of neutrals to the X-point and is even able to suppress flow reversal zones in the hydrogenic flow pattern. Experimentally even more important is the much better pumping found in the case of optimized baffle length (allowing a larger experimental flexibility).

Analyzing the final configuration with respect to impurity compression, one gets a much better compression of helium (an enrichment of helium of typically 2 is now observed in the pumping duct location) than for divertor I (enrichment factors for helium between 0.1 and 0.4). The very good compression of neon in the outside tilted divertor I (enrichment of 1 to 6) is reduced to practically the same as the hydrogen compression (enrichment 1 to 1.5), but is still large enough for an effective feedback control.

This prediction is also a crucial test of the predictive quality of the 2D code used for this study.

References

[1] ITER JCT and Home Teams, Plasma Phys. Control. Fusion 37 (1995) 19.
[2] S.L. Allen et al., J. Nucl. Mater. 196–198 (1992) 804.
[3] M.E. Fenstermacher et al., J. Nucl. Mater. 220–222 (1995) 330.
[4] A. Taroni et al., J. Nucl. Mater. 220–222 (1995) 1086.
[5] H.-S. Bosch et al., Extension of the ASDEX upgrade programme: Divertor II and tungsten target plate experiment; application for prefererttial support, phase I and II, Technical Report 1/281a, IPP, Garching, Germany (1994).
[6] D. Reiter, J. Nucl. Mater. 196–198 (1992) 80.
[7] D. Reiter et al., J. Nucl. Mater. 220–222 (1995) 987.
[8] R. Schneider et al., J. Nucl. Mater. 196–198 (1992) 810.
[9] R. Schneider et al., Contrib. Plasma Phys. 32 (1992) 450, 3rd Workshop on Plasma Edge Theory, Bad Honnef, FRG, June (1992).

[10] H.-S. Bosch et al., 2D model validation of ASDEX-Upgrade scrapeoff layer plasmas, in: Proc. of the 20th EPS Conf. on Controlled Fusion and Plasma Physics, Lisbon (1993), Vol. II (Petit-Lancy, 1993, EPS) pp. 795–798.
[11] H.-S. Bosch et al., J. Nucl. Mater. 220–222 (1995) 558.
[12] D. Coster et al., B2-Eirene modelling of ELMs on ASDEX-Upgrade, in: Proc. of the 21th European Conf. on Controlled Fusion and Plasma Physics, Montpellier, 1994, Vol. II (Petit-Lancy, 1994, EPS) pp. 846–849.
[13] R. Schneider et al., B2-eirene modelling of CDH mode in ASDEX-Upgrade, in: Proc. of the 22nd European Conf. on Controlled Fusion and Plasma Physics, Bournemouth, 1995, Vol. IV (Petit-Lancy, 1995, EPS) pp. 285–288.
[14] D. Coster et al., Self-consistent core and scrape-off-layer modelling, to be published at PSI '96.
[15] J. Neuhauser et al., J. Nucl. Mater. 145–147 (1987) 877.